Zero-bias anomalies and boson-assisted tunneling through quantum dots

Jürgen König[1], Herbert Schoeller[1,2] and Gerd Schön[1]
[1] *Institut für Theoretische Festkörperphysik, Universität Karlsruhe, 76128 Karlsruhe, Germany*
[2] *Department of Physics, Simon Fraser University, Burnaby, B.C., V5A 1S6, Canada*
(June 16, 1995)

We study resonant tunneling through a quantum dot with one degenerate level in the presence of a strong Coulomb repulsion and a bosonic environment. Using a real-time approach we calculate the spectral density and the nonlinear current within a conserving approximation. The spectral density shows a multiplet of Kondo peaks split by the transport voltage and boson frequencies. As a consequence we find a zero-bias anomaly in the differential conductance which can show a local maximum or minimum depending on the level position. The results are compared with recent experiments.

72.15.Qm, 73.20.Dx, 73.40.Gk, 73.50.Fq

Transport phenomena through discrete energy levels in quantum dots have been studied by perturbation theory [1,2] and beyond [3–5]. In general, resonant tunneling phenomena and Kondo effects in nonequilibrium become important, which have been measured recently by Ralph & Buhrman [6]. In metallic islands, the Coulomb blockade is strongly influenced by inelastic interactions with bosonic degrees of freedom, such as fluctuations of the electrodynamic environment [7] or applied time-dependent fields [8]. The study of inelastic interactions in quantum dots with few levels has started only recently, either for the nondegenerate case [9,10] or more general, in the presence of time-dependent fields and Coulomb blockade [2,5]. In earlier work we have studied the influence of bosonic fields in the nonequilibrium Anderson model in the perturbative regime [11] and found resonant side peaks in the Coulomb oscillations.

The purpose of the present letter is to investigate the influence of external quantum-mechanical fields on transport phenomena through ultrasmall quantum dots at low temperatures and frequencies (compared to the intrinsic broadening of the resonant state in the dot). This requires a description of the Kondo effect, generalized to nonequilibrium situations and including coupling to bosonic fields. For the nonperturbative treatment of the tunneling we apply a real-time, nonequilibrium many-body approach developed recently [12,13] to a quantum dot with one level and spin degeneracy M. For $M \geq 2$ and low lying dot level ϵ we obtain the usual Kondo peaks at the Fermi levels μ_α of the reservoirs [4]. However, the emission of bosons causes additional Kondo singularities, for a one mode field at $\mu_\alpha + n\omega_B$ $(n = \pm 1, \pm 2, \ldots)$.

Furthermore, we will analyze the effect of the singularities in the spectral density on the differential conductance as function of the bias voltage. For a low lying level we obtain the well-known zero bias *maximum* [4–6], whereas for a level close to the chemical potentials of the reservoirs we find a zero bias *minimum*. The coupling to bosons gives rise to satellite anomalies, which can be traced back to the corresponding satellite peaks in the spectral density. In a certain range of gate voltages, for $M = 2$ and in the absence of bosons, we find that the temperature and bias voltage dependence of the conductance coincides with recent measurements of zero-bias minima in point-contacts [14]. Therefore, in addition to Refs. [15–17], we propose here another possible interpretation of this experiment.

We consider a dot containing only one energy level with degeneracy M connected via high tunnel barriers to reservoirs of noninteracting electrons. We, furthermore, include a coupling to bosonic modes representing phonons, photons or fluctuations of the electrodynamic environment. Our model Hamiltonian reads $H = H_0 + H_T$, where H_0 describes the decoupled system and H_T the tunneling between leads and dot. We write $H_0 = H_R + H_D$ where $H_R = \sum_{k\sigma\alpha} \epsilon_{k\alpha} a^\dagger_{k\sigma\alpha} a_{k\sigma\alpha}$ refers to the reservoirs (σ and α are spin and reservoir indices). Furthermore, ($\hbar = k_B = 1$)

$$H_D = \epsilon_0 \hat{N} + U_0 \sum_{\sigma<\sigma'} n_\sigma n_{\sigma'} + \sum_q \omega_q d^\dagger_q d_q + \hat{N} \sum_q g_q (d_q + d^\dagger_q) \tag{1}$$

describes the isolated dot with M spin degenerate levels at position ϵ_0, Coulomb repulsion U_0, bosonic modes ω_q and electron-boson coupling g_q. The number of particles on the dot with spin σ is denoted by $n_\sigma = c^\dagger_\sigma c_\sigma$, and $\hat{N} = \sum_\sigma n_\sigma$. Finally, the tunneling term is given by $H_T = \sum_{k\sigma\alpha}(T^\alpha_k a^\dagger_{k\sigma\alpha} c_\sigma + h.c.)$.

This Hamiltonian can be rewritten after a unitary transformation [18] defined by $V = \exp(-i\hat{N}\varphi)$ and $\varphi = i\sum_q (g_q/\omega_q)(d^\dagger_q - d_q)$. We get $\bar{H} = VHV^{-1} = \bar{H}_0 + \bar{H}_T$, where $\bar{H}_0 = H_R + \bar{H}_D$, $\bar{H}_D = \epsilon\hat{N} + U\sum_{\sigma<\sigma'} n_\sigma n_{\sigma'} + \sum_q \omega_q d^\dagger_q d_q$ and $\bar{H}_T = \sum_{k\sigma\alpha}(T^\alpha_k a^\dagger_{k\sigma\alpha} c_\sigma e^{i\varphi} + h.c.)$. Due to the electron-boson interaction the level position and the Coulomb repulsion are renormalized, $\epsilon = \epsilon_0 - \sum_q g_q^2/\omega_q$ and $U = U_0 - 2\sum_q g_q^2/\omega_q$, and the tunneling part contains now phase factors $e^{\pm i\varphi}$.

In lowest order perturbation theory the rates for tunneling in and out of the dot to reservoir α are

$$\gamma^\pm_\alpha(E) = \int dE' \bar{\gamma}^\pm_\alpha(E') P^\pm(E - E') \, , \tag{2}$$

where $\bar{\gamma}^{\pm}_{\alpha}(E) = 1/(2\pi)$, $_{\alpha}(E) f^{\pm}_{\alpha}(E)$ is the classical rate without bosons, , $_{\alpha}(E) = 2\pi \sum_k |T^{\alpha}_k|^2 \delta(E - \epsilon_{k\alpha})$, and $f^{+}_{\alpha}(E)$ is the Fermi distribution of reservoir α with chemical potential μ_α while $f^{-}_{\alpha}(E) = 1 - f^{+}_{\alpha}(E)$. Furthermore, $P^{\pm}(E)$ describes the probability for an electron to absorb (for P^{+}) or emit (for P^{-}) the boson energy E. It is [7]

$$P^{\pm}(E) = \frac{1}{2\pi} \int dt e^{iEt} < e^{i\varphi(0)} e^{-i\varphi(\pm t)} >_0 \qquad (3)$$

where $< ... >_0$ denotes the expectation value with respect to the free boson Hamiltonian. The classical rates together with a master equation are sufficient in the perturbative regime , $= \sum_\alpha$, $_\alpha \ll T$ [11]. In this letter we are interested in temperatures and frequencies which are of the order or smaller than the intrinsic level broadening , , which requires a nonperturbative treatment in , . To achieve this we use a real-time technique developed in [12,13] which provides a natural generalization of the classical and cotunneling theory to the physics of resonant tunneling. For details we refer to these papers. Here we only sketch the derivation and quote the results.

We develop a diagrammatic approach by expanding in the tunneling Hamiltonian $\bar{H}_T$. Since $\bar{H}_0$ contains interaction terms, this can not be done by usual Green's function techniques since Wick's theorem does not apply. However, we can use it with respect to the field operators of the reservoirs, since $\bar{H}_0$ is bilinear in these operators. As an example let us consider the reduced density operator of the dot. We assume that the reservoirs and the boson bath remain in thermal equilibrium. On the other hand, we want to study the nonequilibrium time evolution of the dot. An effective description in terms of the dot degrees of freedom can be derived by expanding all propagators in $\bar{H}_T$ and tracing out the reservoirs by applying Wick's theorem for them. A matrix element of the reduced density operator can then be visualized as shown in Fig.(1).

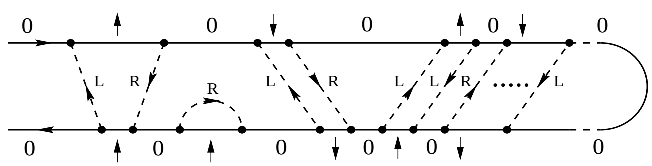

FIG. 1. A diagram showing various tunneling processes: sequential tunneling in the left and right junctions, a term preserving the norm, a cotunneling process, and resonant tunneling.

The forward and the backward propagator (Keldysh contour) are coupled by "tunneling lines" associated with the junctions to each reservoir α. Each tunneling line with energy E represents the rate $\bar{\gamma}^{+}_{\alpha}(E)$ if the line is directed backward with respect to the closed time path and $\bar{\gamma}^{-}_{\alpha}(E)$ if it is directed forward. Because of Fermi-Dirac statistics, we get a factor -1 if two tunneling lines cross each other. The tunneling lines are associated with changes of the state of the dot, as indicated on the closed time path. For large Coulomb repulsion U we can restrict ourselves to states with $N = 0, 1$. The coupling to the bosons is introduced by connecting all vertices in all possible ways by boson lines with a certain energy E (the direction can be chosen in an arbitrary way). The rule for the contribution of the boson lines is exactly the same as for the reservoir lines except that we have to replace $\bar{\gamma}^{\pm}_{\alpha}$ by $P^{\pm}$. Finally, as in the case for metallic islands [12], we have to associate to each tunneling vertex at time t on the contour a factor $\exp i\Delta E t$ where ΔE is the difference of the out- and incoming energies. If the vertex lies on the backward propagator it acquires a factor -1. Analogous graphical rules hold for the Green's functions of the dot as well, the only difference is the occurrence of external vertices.

In leading order, we include only boson lines between vertices which are already connected by tunneling lines. This simply amounts to a dressing of the tunneling lines $\bar{\gamma} \to \gamma$, and the diagrams look identical to those without bosons. The approximation, while neglecting many diagrams, describes well the spectral density of the dot at resonance points. The reason is that position and value of the peaks of the spectral density are determined by a self-energy σ (see Eq. (4)) which is calculated here in lowest order perturbation theory in , including the bosons. Higher orders are small for high tunnel barriers.

Similar to the case of metallic islands [12,13] we proceed in a conserving approximation, which takes into account non-diagonal matrix elements of the total density matrix up to the difference of one electron-hole pair excitation in the reservoirs. The difference in the case of a single level quantum dot is that we have now M possibilities for the occupied state. The analytic resummation of the corresponding diagrams yields for the transitions between $N = 0(1)$ and $1(0)$ the rates $\Sigma^{\pm} = \lambda \int dE \gamma^{\pm}(E) |R(E)|^2$. Here $R(E) = [E - \epsilon - \sigma(E)]^{-1}$ defines a resolvent with broadening and energy renormalization given by the self-energy

$$\sigma(E) = \int dE' \frac{M\gamma^{+}(E') + \gamma^{-}(E')}{E - E' + i0^{+}} \qquad (4)$$

where $\gamma^{\pm} = \sum_\alpha \gamma^{\pm}_\alpha$ and $\lambda^{-1} = \int dE |R(E)|^2$.

In the classical limit , $<< T$ we recover for $\Sigma^{\pm}$ the classical rates $\gamma^{\pm}$. The stationary probabilities P_0 and P_1 for an unoccupied or occupied dot state follow from the kinetic equation which uses the rates as input $P_1 \Sigma^{-} - P_0 M \Sigma^{+} = 0$. Together with $P_0 + P_1 = 1$ we obtain $P_0 = \int dE \gamma^{-}(E) |R(E)|^2$ and $P_1 = M \int dE \gamma^{+}(E) |R(E)|^2$.

Summing equivalent diagrams for the real-time Green's functions of the dot we obtain the spectral density $\rho \equiv (G^{<} - G^{>})/(2\pi i)$

$$\rho(E) = \int dE' \sum_{r=\pm} \gamma^{r}(E') P^{-r}(E' - E) |R(E')|^2 \qquad (5)$$

and for the current I_α flowing into reservoir α

$$I_\alpha = e2\pi M \sum_{\alpha'} \int dE' \sum_{r=\pm} r\gamma_\alpha^{-r}(E')\gamma_{\alpha'}^r(E')|R(E')|^2. \quad (6)$$

For the special case of two reservoirs $\alpha = L/R$ and constant level broadening , $=$, $_L$ $=$, $_R$ the current $I = I_L = -I_R$ can be written as

$$I = e\frac{M}{2}, \int dE\rho(E)[f_R^+(E) - f_L^+(E)]\,. \qquad (7)$$

Our results satisfy all sum rules together with current conservation, and one can prove particle-hole symmetry in the case $M = 1$.

The difference to other approaches in the $M = 1$ case [9,10] is clearly displayed by the effect of the self-energy $\sigma(E)$ which determines via the resolvent $R(E)$ the position of the maxima of the spectral density (5). In all previous works, $\sigma(E)$ has been approximated by a constant. We find that the energy dependence of $\sigma(E)$ cannot been neglected if the temperature T and the typical frequency ω_B of the bosons are smaller than , . To derive this analytically we consider from now on a one-mode environment (Einstein model) with boson frequency $\omega_q = \omega_B$. Defining $g = \sum_q g_q^2/\omega_B^2$ we obtain $P^\pm(E) = \sum_n p_n\delta(E \pm n\omega_B)$, where $p_n = e^{-g(1+2N_0)}e^{n\omega_B/2T_B}I_n(2gN_0e^{\omega_B/2T_B})$ is the probability for the emission of n bosons with frequency ω_B. Here, N_0 is the Bose function, I_n denotes the modified Bessel function. The temperature of the boson bath is T_B. In real experiments it can be different from the electron temperature T. Using (2) and (4) we obtain

$$Re\,\sigma(E) = \sum_{n,\alpha}(Mp_n - p_{-n})\frac{,}{2\pi}\left[ln\left(\frac{E_C}{2\pi T}\right)\right.$$
$$\left. -Re\,\Psi\left(\frac{1}{2} - i\frac{E + n\omega_B - \mu_\alpha}{2\pi T}\right)\right] \qquad (8)$$

and $Im\,\sigma(E) = -\pi\sum_n p_n[M\bar\gamma^+(E + n\omega_B) + \bar\gamma^-(E - n\omega_B)]$. Here Ψ denotes the digamma function, and we have chosen in the energy integrals a Lorentzian cut-off at E_C. The real part of σ depends logarithmically on energy, temperature, voltage and frequency. These logarithmic terms are typical for the occurrence of Kondo peaks and do not cancel for $M \geq 2$ or $p_n \neq p_{-n}$. Hence we anticipate logarithmic singularities not only for the degenerate case but also for a single dot level without spin since the probabilities for absorption and emission of bosons are different. This is an important difference to the case of classical time-dependent fields [5] where both probabilities are equal.

Fig. (2) shows a typical series of pictures for the spectral density at different voltages for a low lying level ϵ. Without bias and $M = 2$, we obtain the usual Kondo peak near the Fermi level (which we choose as zero energy). Due to emission of bosons, there are now additional resonances at multiples of ω_B. For finite bias voltage, all peaks split and decrease in magnitude.

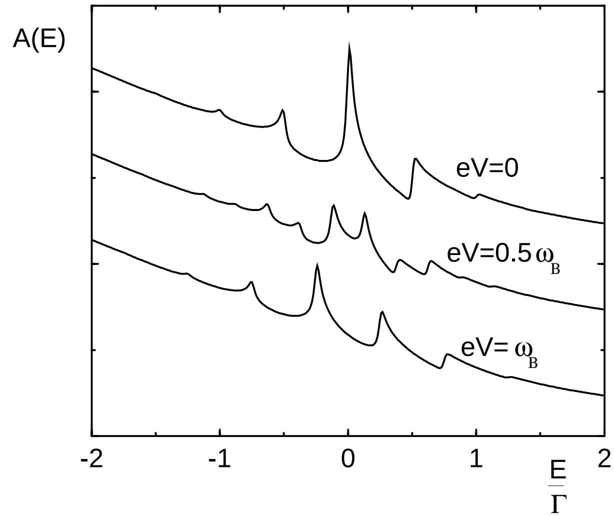

FIG. 2. The spectral density for $T = T_B = 0.01,$, $\epsilon = -4,$, $g = 0.2$, $\omega_B = 0.5$, and $E_C = 100$, at different voltages. For $V = 0$ there are resonances at multiples of ω_B, which split for finite bias voltage.

The resonances in the spectral density can be seen most pronounced in the nonlinear differential conductance as function of the bias voltage V. Fig. (3) shows the differential conductance for a low lying level ϵ.

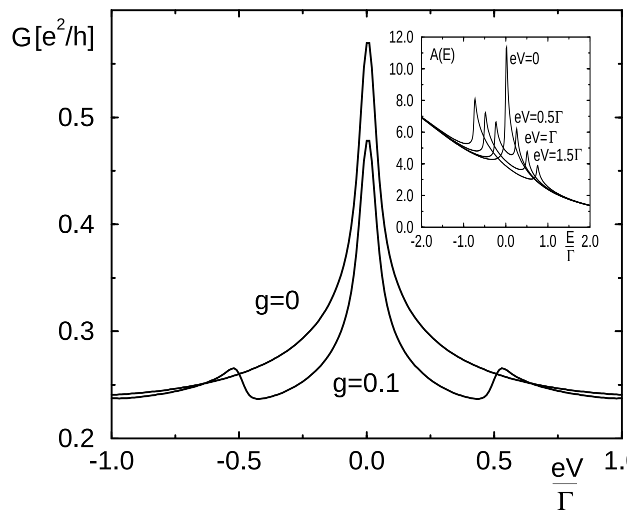

FIG. 3. The differential conductance vs. bias voltage for $T = T_B = 0.01,$, $\epsilon = -4,$, $\omega_B = 0.5$, and $E_C = 100,$. The curves show a maximum at zero bias and satellite maxima at multiples of ω_B for a finite electron-boson coupling. Inset ($g = 0$): increasing voltage leads to an overall decrease of the spectral density in the range $|E| < eV$, which explains the zero-bias maximum.

As usual we find a zero-bias maximum [4–6] since the splitting of the Kondo peak leads to an overall decrease of the spectral density in the energy range $|E| < eV$ (see inset of Fig. (3)). Due to emission of bosons we observe also a set of symmetric satellite maxima. They can be traced back to the fact that pairs of Kondo peaks can merge if the bias voltage is given by multiples of the boson frequency (see Fig. (2)). This gives rise to pronounced Kondo peaks at $E = \pm eV/2$ and thus to an increase of the spectral density with bias voltage near these points.

The differential conductance for ϵ near zero energy is shown in Fig. (4) with and without bosons. Surprisingly we find that the whole structure is inverted compared to the $\epsilon < 0$ case and we find a zero-bias anomaly although the Kondo peak at zero energy is absent. The contributions of sequential and cotunneling lead only to an overall shift of the differential conductance without any interesting structure. This shows clearly that the influence of the logarithmic terms in $\sigma(E)$ is still important. They lead to an overall increase of the spectral density near zero energy with bias voltage. In the presence of bosons we obtain satellite steps at $|eV| = m\omega_B$.

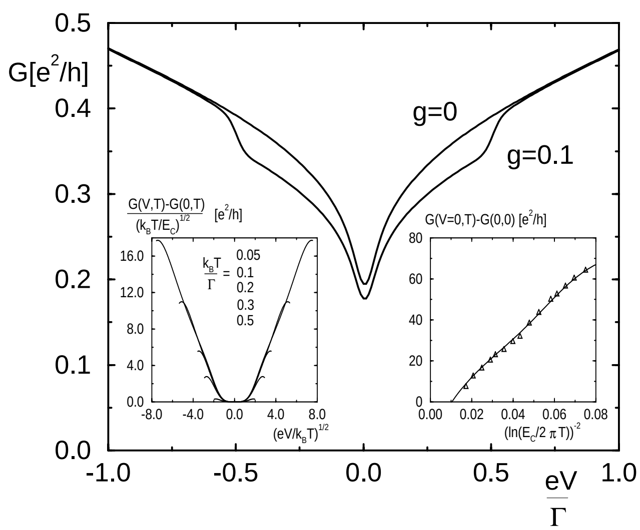

FIG. 4. The differential conductance vs. bias voltage for $T = T_B = 0.01$, , $\epsilon = 0$, $\omega_B = 0.5$, and $E_C = 100$, . The curves show a minimum at zero bias and steps at multiples of ω_B for a finite electron-boson coupling. Left inset: the rescaled curves for $g = 0$ at different temperatures collapse onto one curve. Right inset: The temperature dependence of the linear conductance (solid line) coincides with experimental data from [14] (triangles).

The occurrence of zero-bias minima is well known for Kondo scattering from magnetic impurities [19]. Here we have shown that zero-bias minima can also occur by resonant tunneling via local impurities if the level position is high enough to enter the mixed valence regime. We have also compared the scaling behavior of the conductance as function of temperature and bias voltage with recent experiments of Ralph & Buhrman [14] (see insets of Fig. (4)). The coincidence is quite remarkable. The explanation of this experiment, either interpreting it as 2-channel Kondo scattering from atomic tunneling systems [15,16] or by tunneling into a disordered metal [17], is still controversial. The mechanism described in this work offers another possibility although the magnetic field dependence of the experiments remains unexplained.

Finally, we also investigate the differential conductance at fixed bias voltage as function of the position of the dot level, which experimentally can be varied by changing the gate voltage coupled capacitively to the dot. Fig. (5) shows the classically expected pair of peaks at $|\epsilon| = eV/2$ together with satellites between the main peaks (due to emission and absorption) and peaks for $|\epsilon| > eV/2$ (only due to absorption of bosons).

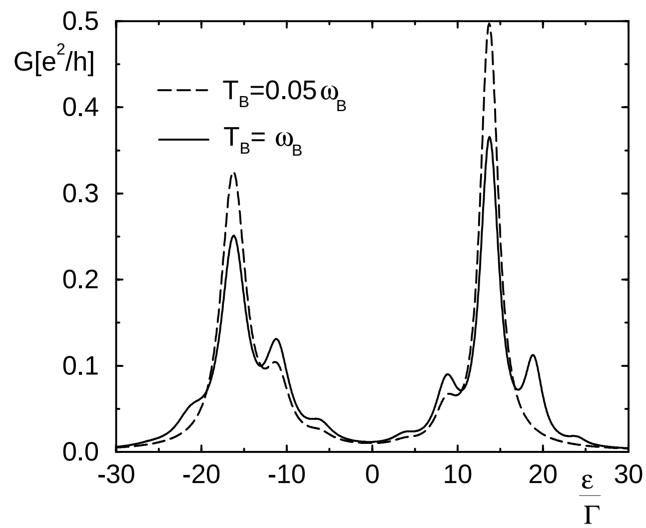

FIG. 5. The differential conductance as a function of ϵ for $T = 0.25$, , $eV = 30$, , $g = 0.3$, $\omega_B = 5$, and $E_C = 500$, .

The imaginary part of $\sigma(E)$ gives rise to a classically unexpected asymmetry of the peak heights. The peak at $\epsilon = eV/2$ is larger than the one at $\epsilon = -eV/2$ since $|Im\,\sigma(E)| = \pi|M\gamma^+(E) + \gamma^-(E)|$ is always smaller for higher energies (except for the $M = 1$ case where particle-hole symmetry holds). This demonstrates a significant effect due to the broadening of the spectral density by quantum fluctuations.

In conclusion, we have studied for the first time low-temperature transport in the nonequilibrium Anderson model with bosonic interactions. A one-mode environment yields new Kondo resonances in the spectral density which can be probed by the measurement of the nonlinear differential conductance. We have shown that both the gate and bias voltage dependence is important. Quantum fluctuations due to resonant tunneling yield zero-bias anomalies as function of the bias voltage, which can be changed from maxima to minima by varying the gate voltage. We found similarities to recent experiments.

We like to thank D. Averin, J. von Delft and M. Hettler for useful discussions. Our work was supported by the "Deutsche Forschungsgemeinschaft" as part of "SFB 195" and the Swiss National Science Foundation (H.S.).

---

[1] D.V. Averin, A.N. Korotkov, and K.K. Likharev, Phys. Rev. **B44**, 6199 (1991); C.W.J. Beenakker, Phys. Rev. **B44**, 1646 (1991); L.I. Glazman and K.A. Matveev, JETP Lett **48**, 445 (1988).

[2] C. Bruder and H. Schoeller, Phys. Rev. Lett. **72**, 1076 (1994).

[3] T.K. Ng and P.A. Lee, Phys. Rev. Lett. **61**, 1768 (1988); L.I. Glazman and M.E. Raikh, JETP Lett. **47**, 452 (1988); S. Hershfield, J.H. Davies, and J.W. Wilkins, Phys. Rev. Lett. **67**, 3720 (1991)

[4] Y. Meir, N.S. Wingreen, and P.A. Lee, Phys. Rev. Lett. **70**, 2601 (1993); N.S. Wingreen and Y. Meir, Phys. Rev. **B49**, 11040 (1994).

[5] M.H. Hettler and H. Schoeller, to appear in Phys. Rev. Lett.

[6] D.C. Ralph and R.A. Buhrman, Phys. Rev. Lett. **72**, 3401 (1994).

[7] M.H. Devoret et al., Phys. Rev. Lett. **64**, 1824 (1990); S.M. Girvin et al. Phys. Rev. Lett. **64**, 3183 (1990); A.A. Odintsov, Sov. Phys. JETP **67**, 1265 (1988); A.A. Odintsov, V. Bubanja, and G. Schön, Phys. Rev. **B46**, 6875 (1992); K. Flensberg *et al.*, Phys. Scripta **T42**, 189 (1992).

[8] L.P. Kouwenhoven *et al.*, Phys. Rev. **B50**, 2019 (1994); I.A. Devyatov and K.K. Likharev, Physica **B194-196**, 1341 (1994);

[9] N.S. Wingreen, K.W. Jacobsen, and J.W. Wilkins, Phys. Rev. Lett. **61**, 1396 (1988); L.I. Glazman and R.I. Shekhter, Sov. Phys. JETP **67**, 163 (1988); M. Jonson, Phys. Rev. **B39**, 5924 (1989).

[10] H.T. Imam, V.V. Ponomarenko, and D.V. Averin, Phys. Rev **B50**, 18288 (1994).

[11] J. Stampe, H. Schoeller, unpublished.

[12] H. Schoeller and G. Schön, Phys. Rev. **B50**, 18436 (1994); Physica **B203**, 423 (1994).

[13] J. König, H. Schoeller and G. Schön, to be published in Europhys. Lett.; J. König, H. Schoeller, G. Schön and R. Fazio, in *Quantum Dynamics of Submicron Structures*, eds. H. A. Cerdeira et al., NATO ASI Series E, Vol. 291 (Kluwer, 1995), p.221

[14] D.C. Ralph and R.A. Buhrman, Phys. Rev. Lett. **69**, 2118 (1992); Phys. Rev. **B51**, 3554 (1995).

[15] D.C. Ralph, A.W.W. Ludwig, J. von Delft and R.A. Buhrman, Phys. Rev. Lett. **72**, 1064 (1994).

[16] M.H. Hettler, J. Kroha, and S. Hershfield, Phys. Rev. Lett. **73**, 1967 (1994).

[17] N.S. Wingreen, B.L. Altshuler and Y. Meir, unpublished.

[18] G.D. Mahan, *Many-Particle Physics*, (Plenum, 1990).

[19] A.G.M. Jansen, A.P. van Gelder, P. Wyder, and S. Strassler, J. Phys. **F11**, L15 (1981).